Numerical Simulation for Pressure Distribution in Pelton Turbine Nozzle for the Different Shapes of Spear

Abhishek Sharma
Department of Mechanical Engineering, Rajiv Gandhi Proudyogiki Vishwavidyalaya, Bhopal, (MP)

Prashant Sharma
Department of Mechanical Engineering, Rajiv Gandhi Proudyogiki Vishwavidyalaya, Bhopal, (MP)

Anil Kothari
Department of Training and Placement, Rajiv Gandhi Proudyogiki Vishwavidyala Bhopal, (MP)

Abstract **This Paper Present a simulation for design of spear for nozzle by applying computational fluid dynamics analysis and using ANSYS software. With the development of high speed computers and advancement in numerical techniques detail flow analysis of the desired model can be done for design optimization. The design can be altered till the best performance or desired output is obtained. This is less time consuming.**

CFD can provide the solution for different operating condition and geometry configuration in less time and cost and found very useful for design and development.

In the present work, three shapes of spear at different mass flow rates have been analysed using ANSYS-CFX 10 software, the pressure and velocity distribution are obtained and compared. Using the analysis result, the loss variations with the nozzles for different spear shapes are computed. The results are presented in tabular and graphical form.

Key Words: Numerical Modeling, Pelton wheel nozzle, Spear design

I. INTRODUCTION

Hydraulic turbines have a series of blades fitted to wheel mounted on a rotating shaft.. Flowing water is directed on to the blades of a turbine runner, creating a force on the blade since the runner is spinning in this way energy is transferred from the water flow to the turbine The velocity and pressure of the liquid reduce while flowing through the hydraulic turbines.

II. PELTON TURBINE

The Pelton wheel is among the most commonly used turbine for high head power plant. The Pelton wheel extract energy due to change of impulse (momentum) of moving water, as opposed to its weight like traditional overshot water wheel. Although many variations of impulse turbines existed prior to Pelton design, they were less efficient than Pelton's design, the water leaving these wheels typically still had high speed, and carried away much of the energy. Pelton' paddle geometry was designed so that when the rim runs at ½ the speed of the water jet, the water leaves the wheel with very little speed, extracting almost all of its energy, and allowing for a very efficient turbine. The runner consists of a circular disk with a buckets evenly spaced round its periphery. The buckets have a shape of double semi-ellipsoidal cups. Each bucket is divided into symmetrical parts by a sharp-edged ridge known as splitter.

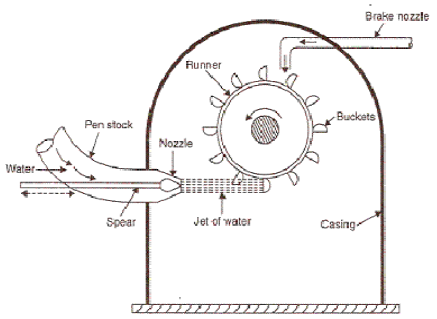

Fig. 1. Spear controlling the jet striking Pelton Wheel.

III. PRINCIPLES OF FLUID FLOW

There are three basic principles of fluid flow

Principle of Conservation of Mass – It states that *"Mass can neither be created nor destroyed"*. Continuity equation has been derived on this principle.

Principle of Conservation of Energy – It states that *"Energy can neither be created nor destroyed"*. On the basis of this principle the energy equation is derived.

Principle of Conservation of Momentum – It states that *"The impulse of the resultant force, or the product of the force and time increment during which it acts is equal to change in momentum of the body"*. Momentum equation is derived on this basis.

- **Continuity Equation**

The rate of increase of the fluid mass contained within the region must be equal to the difference between the rate at which the fluid mass enters the region and the rate at which the fluid mass leaves the region. However, if the flow is steady, the rate of increase of fluid mass within the region is equal to zero, then the rate at which the fluid mass enters the region is equal to the rate at which the fluid mass leaves the region.

$$\frac{\partial \rho}{\partial t} + \frac{\partial (\rho V_x)}{\partial x} + \frac{\partial (\rho V_y)}{\partial y} + \frac{\partial (\rho V_z)}{\partial z} = 0$$

- **Momentum Equation**

According to Newton's Second Law of motion, inertia force acting on a body in any direction is equal to resultants of all body and surface forces in that direction.

$$\frac{\partial V_x}{\partial t} + V_x \frac{\partial V_x}{\partial x} + V_y \frac{\partial V_y}{\partial y} + V_z \frac{\partial V_z}{\partial z} = F_x - \frac{1}{\rho}\frac{\partial P}{\partial x} + \frac{\mu}{\rho}\left(\frac{\partial^2 V_x}{\partial x^2} + \frac{\partial^2 V_x}{\partial y^2} + \frac{\partial^2 V_x}{\partial z^2}\right)$$

$$\frac{\partial V_y}{\partial t} + V_x \frac{\partial V_y}{\partial x} + V_y \frac{\partial V_y}{\partial y} + V_z \frac{\partial V_y}{\partial z} = F_y - \frac{1}{\rho}\frac{\partial P}{\partial x} + \frac{\mu}{\rho}\left(\frac{\partial^2 V_y}{\partial x^2} + \frac{\partial^2 V_y}{\partial y^2} + \frac{\partial^2 V_y}{\partial z^2}\right)$$

$$\frac{\partial V_z}{\partial t} + V_x\frac{\partial V_z}{\partial x} + V_y\frac{\partial V_z}{\partial y} + V_z\frac{\partial V_z}{\partial z} = F_z - \frac{1}{\rho}\frac{\partial P}{\partial x} + \frac{\mu}{\rho}\left(\frac{\partial^2 V_z}{\partial x^2} + \frac{\partial^2 V_z}{\partial y^2} + \frac{\partial^2 V_z}{\partial z^2}\right)$$

- **Energy Equation**

Energy equation is obtained by multiplying the equation of momentum by velocity components in each coordinate direction and then adding and integrating over the volume.

$$\int_{\forall}\frac{\rho}{2}\left(\frac{\partial V^2}{\partial t} + V_x\frac{\partial V^2}{\partial x} + V_y\frac{\partial V^2}{\partial y} + V_z\frac{\partial V^2}{\partial z}\right)d\forall$$
$$= \int_{\forall}(F_xV_x + F_yV_y + F_zV_z)d\forall + \int_{\forall}[V_x\left(\frac{\partial \sigma_x}{\partial x} + \frac{\partial \tau_{xy}}{\partial y} + \frac{\partial \tau_{xz}}{\partial z}\right)$$
$$+ V_y\left(\frac{\partial \sigma_y}{\partial y} + \frac{\partial \tau_{yx}}{\partial x} + \frac{\partial \tau_{yz}}{\partial z}\right) + V_z\left(\frac{\partial \sigma_z}{\partial z} + \frac{\partial \tau_{zy}}{\partial y} + \frac{\partial \tau_{zx}}{\partial x}\right)]d\forall$$

IV. FLOW THROUGH NOZZLE

A nozzle is a gradually converging short tube which is fitted at the outlet and of the penstock for the purpose of converting the total energy of the flowing water into kinetic energy. Nozzles are used where high velocities of flow are required to be developed. In impulse turbines, it is required to convert whole of hydraulic energy into kinetic energy.

The discharge is given by,

$$Q = a_1v_1 = a_2v_2 \ldots\ldots\ldots\ldots\ldots\ldots\ldots\ldots (i)$$

The nozzle is horizontal and the nozzle axis is assumed as datum for elevation and hence head at nozzle is given by,

$$H = \frac{v^2}{2g} + \frac{p}{\gamma} \ldots\ldots\ldots\ldots\ldots\ldots\ldots\ldots (ii)$$

Head loss in nozzle is given by,

$$H_l = H_1 - H_2 \ldots\ldots\ldots\ldots\ldots\ldots\ldots\ldots (iii)$$

Head loss coefficient is given by,

$$\Psi c = H\,l/H1 \ldots\ldots\ldots\ldots\ldots\ldots\ldots\ldots (3)$$

Coefficient of discharge is given by,

$$C_d = \frac{Q\sqrt{a_1^2 - a_2^2}}{a_1a_2\sqrt{2gH_1}} \ldots\ldots\ldots\ldots\ldots\ldots\ldots\ldots (v)$$

Coefficient of pressure is given by,

$$C_p = \frac{p_1 - p_2}{\frac{1}{2}\rho v_2^2} \quad \ldots\ldots\ldots\ldots\ldots\ldots\ldots\ldots\ldots\ldots\ldots\ldots\ldots\ldots (vi)$$

Coefficient of velocity is given by,

$$C_v = \frac{v_2}{\sqrt{2gH_1}} \quad \ldots\ldots\ldots\ldots\ldots\ldots\ldots\ldots\ldots\ldots\ldots\ldots\ldots\ldots (vii)$$

V. COMPUTATIONAL FLUID DYNAMICS

Computational fluid dynamics (CFD) is one of the branches of fluid mechanics that uses numerical methods and algorithms to solve and analyze problems that involve fluid flows. Computers are used to perform the millions of calculations required to simulate the interaction of liquids and gases with surfaces defined by boundary conditions. Even with high-speed supercomputers only approximate solutions can be achieved in many cases. Ongoing research, however, may yield software that improves the accuracy and speed of complex simulation scenarios such as transonic or turbulent flows. Initial validation of such software is often performed using a wind tunnel with the final validation coming in flight test.

VI. GEOMETRIC MODELING

The modeled assembly of nozzle for pelton turbine consists of nozzle (pipe of converging cross-sectional area), spear and a free surface flow domain. The modeled assembly consists of inlet, nozzle, spear and outlet. The modeled assembly of free surface flow domain consists of extended outlet. The modeling has been done in ANSYS Workbench 10 and ANSYS ICEM CFD 10. The 3D-view of spear is shown in Fig.2.

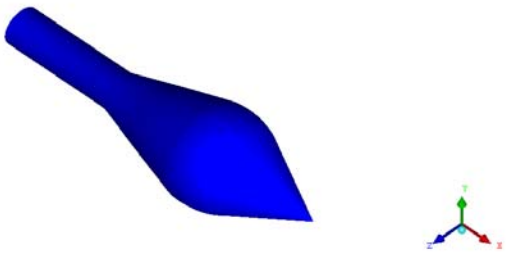

Isometric view of 1st spear

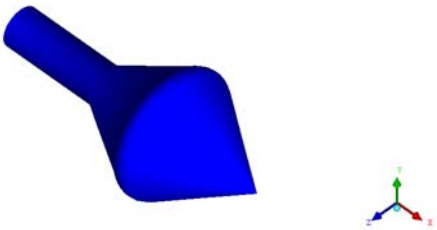

Isometric view of 2nd spear

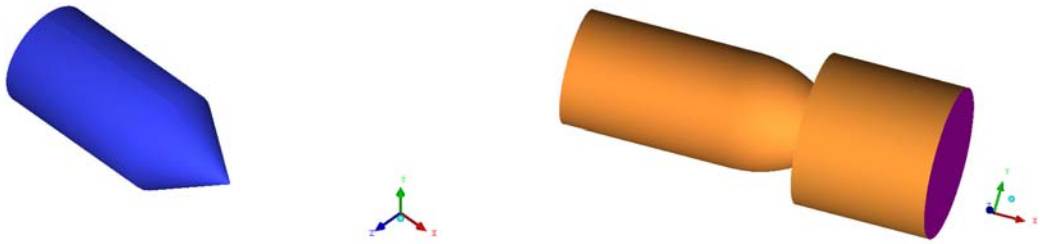

Isometric View of 3rd spear *Complete isometric view of the nozzle , spear and free surface flow*

Fig.2.

VII. MESH GENERATION

The geometry made is divided into small sub parts for CFD analysis called mesh and the process is called meshing. The shape of the mesh elements can be triangular, quadrilateral, tetrahedral, hexahedral or prism depending upon the size and shape of the geometry. The shape and size of the mesh elements can be varied and are kept according to the dimension of the geometry, accuracy required, computational power of the system and memory. The complete nozzle flow space is divided into two domains and the mesh is generated.

The meshing of nozzle and spear domain has been done at different spear shapes and the meshing of nozzle spear domain for fillet spear shape has been shown in fig.
The summary of meshing data for each surface has been described in table.

Table. 1. Mesh Data for Nozzle Spear Domain.

Part name	*A. No. of Elements*	*B. Element Type*
Inlet	2812	Triangle
Outlet	727	Triangle
Spear	102597	Triangle
Nozzle	380122	Triangle
Extended	343343	Tetrahedral
Extended outlet	4184	Tetrahedral

(first spear)

Table 2. Mesh Data for Nozzle Spear Domain. (second spear).

Part name	*C. No. of Elements*	*D. Element Type*
Inlet	5100	Triangle
Outlet	1350	Triangle
Spear	98091	Triangle
Nozzle	445457	Triangle
Extended	434330	Tetrahedral
Extended outlet	8193	Tetrahedral

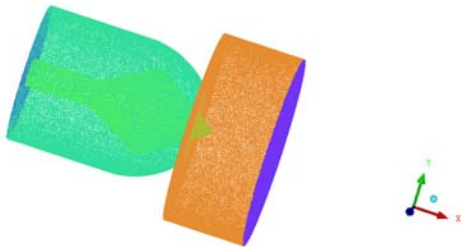

Table 3. Mesh Data for Nozzle Spear domain third SPEAR.

Part name	*E. No. of Elements*	*F. Element Type*
Inlet	3295	Triangle
Outlet	1350	Triangle
Spear	184614	Triangle
Nozzle	417295	Triangle
Extended	434125	Tetrahedral
Extended outlet	8121	Tetrahedral

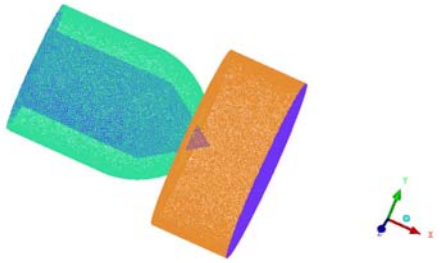

VIII. DOMAIN AND INTERFACE PROPERTIES

The mesh is converted into the required format and is imported to ANSYS CFX-10 software. In ANSYS CFX-Pre the properties of the domains and fluid are defined along with their interface properties. The summary of the domain 1 properties are given in table 4.

Table 4. Domain 1 Properties.

Location	Fluid
Domain Type	Fluid Domain
Fluid List	Water
Coordinate Frame	Coord 0
Reference Pressure	1 [atm]
Buoyancy Option	Not Buoyant
Domain Motion Option	Stationary
Mesh Deformation Option	None
Heat Transfer Option	Isothermal
Fluid Temperature	25^0[C]
Turbulence Model	k-Epsilon
Turbulence Wall Function	Scalable
Density of Water	997 kg/m^3
Kinematic Viscosity of water	0.8926X $10^{-6} m^2/s$

Domain 2 Properties

Location	Fluid 2
Domain Type	Fluid Domain
Fluid List	Water
Coordinate Frame	Coord 0
Reference Pressure	1 [atm]
Buoyancy Option	Not Buoyant
Domain Motion Option	Stationary
Mesh Deformation Option	None
Heat Transfer Option	Isothermal
Fluid Temperature	25^0[C]
Turbulence Model	k-Epsilon
Turbulence Wall Function	Scalable

IX. BOUNDARY CONDITIONS

The boundary conditions are applied at the inlet and outlet surfaces of the domains.

Inlet Boundary Condition: The mass flow rate and its direction with normal direction to the inlet surface i.e., at inlet of nozzle domain is applied. Turbulence is set to medium intensity (upto 5%).

Outlet Boundary Condition: The reference pressure at the outlet of the external domain was set equal to 1 atmospheric.

Wall Conditions: The walls of all the domains are assumed to be smooth and no slip condition is assigned.

Turbulence Model: k- Є model used

Solver

Specific Blend Factor with 0.9 value has been used for up to 200 iterations. The timescale control is set to Auto Timescale. The RMS residual target has been set to 1x10E-7 for termination of the calculations.

Post Processing

3D-Streamlines of velocity and pressure contours starting from inlet of the nozzle can be seen in all the domains. Using the function calculator in tools average values of various parameters like the velocity, pressure, area, mass flow rate at the boundaries and the required domain can be found out for computation of loss, pressure and velocity coefficients.

X. PRESSURE DISTRIBUTION ACROSS CROSS SECTION AREA

The pressure distribution across the flow area are obtained on two planes one plane is at the interface of outlet of nozzle and second plane is created at the highest curvature point of spear and applying for pressure contour and putting transparency value is 0.1 so in different color scheme pressure contour is find out with the help of this pressure contour we can find out pressure distribution on that plane.

First Spear

In the first spear we are making the plane at the distance of 0.7 m and putting pressure contour with transparency value 0.1.

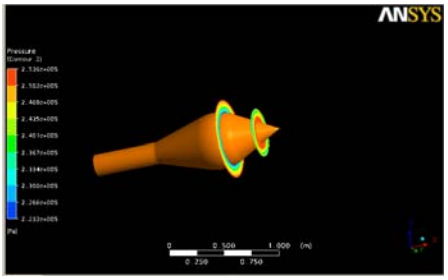

Pressure contour at the plane for mass flow rate 2412.74 kg/s

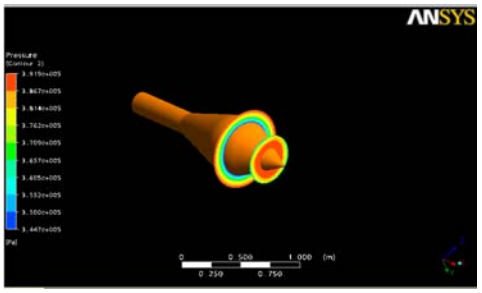

Pressure contour at plane for the mass flow rate 3015.93 kg/s

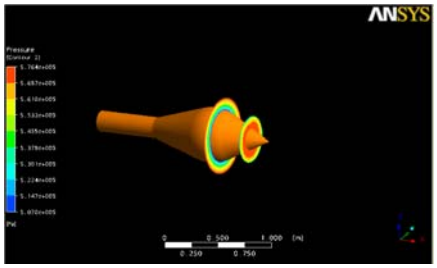

Pressure contour at plane for the mass flow rate 3619.11 kg/s

These pressure contour shows that the plane at the interface of nozzle and extended surface domain having higher pressure distribution at the inner periphery compare to outer periphery of the plane, and the plane at the highest curvature point having higher pressure distribution at the outer periphery of plane and minimum at the inner periphery.

Second Spear

In the second spear we are making the plane at the distance of 0.4 m and putting pressure contour with transparency value 0.1

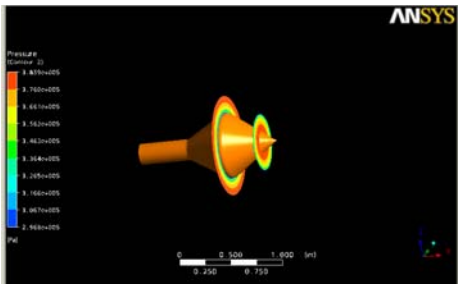

Pressure contour at plane for the mass flow rate 3952.121 kg/s.

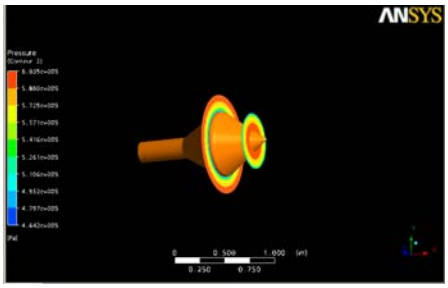

Pressure contour at plane for the mass flow rate 4940.15 kg/s.

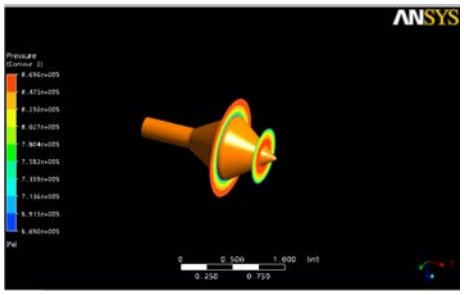

Pressure contour at plane for the mass flow rate 5928.18 kg/s.

These three pressure contour having pressure distribution in the same fashion as the pervious spear accepting that value of pressure is comparatively high.

Third Spear

In the third spear we are making the plane at the distance of -0.3 m and putting pressure contour with transparency value 0.1

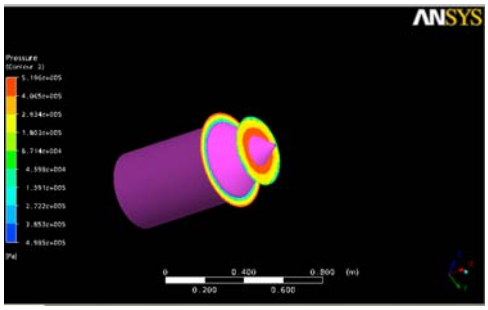

Pressure contour at plane for the mass flow rate 3952.12kg/s.

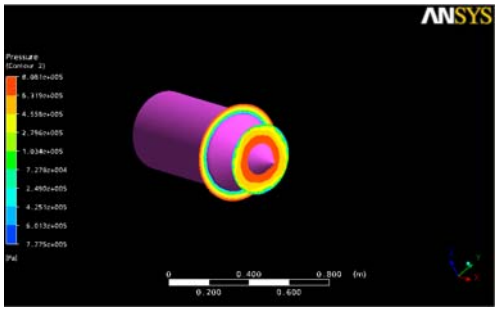

Pressure contour at plane for the mass flow rate 4940.15kg/s.

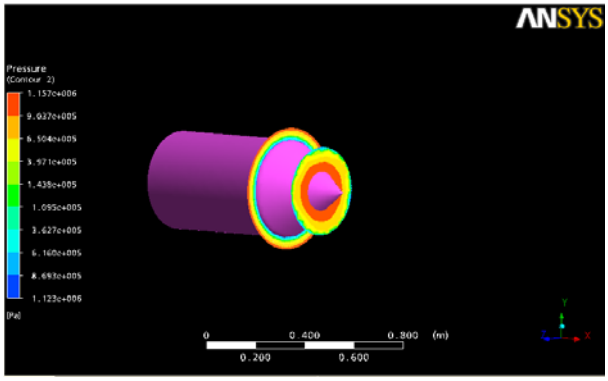

Extra plane pressure contour at mass flow rate 5928.18 kg/s.

At the interface region these three pressure contour having long strip of yellow color in the middle portion of periphery of plane that shows moderate value of pressure for very long time then small increment in pressure shown by red strip at the inner periphery of plane.
And pressure distribution for plane at the highest curvature point location varying as at the inner periphery of plane pressure contour showing blue strip and changes to yellow and finally end at the outer periphery with red color that shows pressure is continuously changing and max for outer periphery. Fig (6.28, 6.29, 6.30)

Different Spear with Same Mass Flow Rate

For finding out pressure distribution changes due to change of design of spear at interface of nozzle and extended surface domain and at the highest curvature point of spear this analysis carried out.
In this analysis take the three different spears at same mass flow rate of 3500 kg/sec and transparency value kept constant at 0.1.

Result for first spear

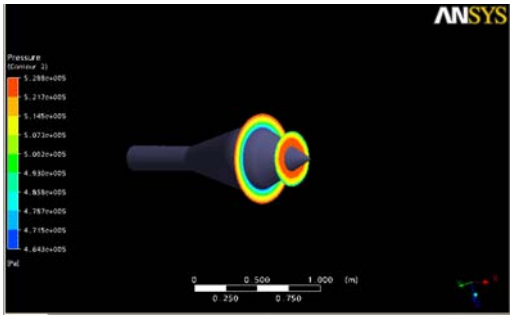

Pressure contour for first spear at plane for the mass flow rate 3500 kg/sec.

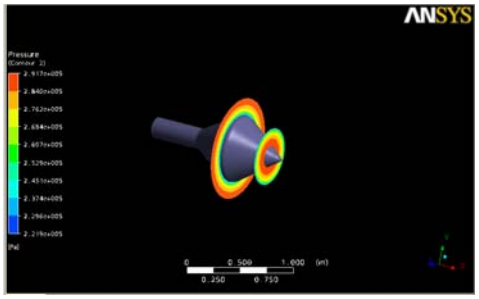

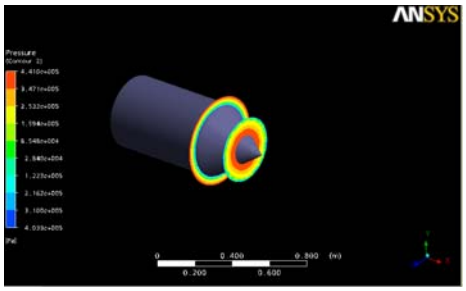

Second spear **Third spear mass flow rate 3500kg/sec**

This pressure contour shows that at the plane of interface location pressure distribution is higher at the inner periphery of plane for second spear.
And plane at the highest curvature point location pressure distribution is max at outer periphery of plane of second spear.

XI. CONCLUSION

In this dissertation Computational Fluid Dynamics (CFD) approach has been used to predict the performance of different shape of spear at different mass flow rates and nozzle openings.
The pressure at the inlet of the nozzle and spear increases with the increase in mass flow rate for the same spear shape .The pressure is maximum for the second spear and nozzle geometry at the 5928.18 kg/sec mass flow rate at the inlet and it is minimum for the first spear and nozzle with 3952.12 kg/sec mass flow rate. The pressure at the . outlet is nearly equal to atmosphere as the jet is issued freely in air. The outlet velocity of the jet is higher than the inlet velocity of the fluid which shows that the pressure energy is being converted into kinetic energy. The coefficient of pressure is max for second spear (0.9608) having mass flow rate 3952.12 kg/sec. The velocity increases with the increase in mass flow rates from 3952.12 to 5928.18 kg/sec at the inlet and at the outlet for all spear because of constant area. The coefficient of velocity is maximum for the first spear (0.8998) having 4940.15 kg/sec mass flow rate. The coefficient of discharge is maximum for the first spear (0.789755) having 4940.15 kg/sec mass flow rate. The streamlines converge slowly for third shape spear nozzle geometry but for second and first spear nozzle geometry streamlines converge sharply as these has sharp curvature as seen in figures.
Due to sharp curvature, the pressure at outlet of the third spear nozzle geometry is more than the pressure at outlet of the first and second spear geometry.
The third spear nozzle geometry has the highest head loss coefficient (0.0310) among all the three geometry.From the streamlines, it is seen that the jet coming out of 1st and 2nd spear and nozzle diverges as seen in Figure but the jet coming out of 3rd spear nozzle remains compact as seen in Figures (Vena-contracta can be seen in velocity streamlines when the jet of water just leaves the nozzle as seen in Figures) The computation and comparison of different flow coefficients of various geometric configurations using CFD will help to optimize the nozzle and spear shape.
In present case it may be concluded that 1st spear is better than the other two spears.

Pressure Distribution Across Cross Section Area

It is observed that pressure is highest at inner periphery and decreases towards outer side,
The pressure distribution on a plane at the highest curvature point of spear shows that pressure is minimum at the inner periphery and increases towards outer periphery.
It is also seen that as the mass flow rate increases pressure values at any point on any cross section area increases.

REFERENCES

[1] W.A.Doble (1899), "*The Tangential Water Wheel*", Transaction of the American Institute of Mining Engineers, Vol. 29, pp.852-858
[2]W Malalasekera and H K Versteeg (1995), "*An Introduction to Computational Fluid Dynamics*", the Finite Volume Method, Longman
[3]W.N. Dawes (1998), "*Computational Fluid Dynamics for Turbomachinery Design*", Whittle Laboratory, Department of Engineering, University of Cambridge, UK
[4]Kearon Bennet, Jacek Swiderski, Jinxing Huang (2000), "*Application of CFD Turbine Design for Small Hydro Elliott Falls, A Case Study*", Transaction of SECFD, Ottawa engineering limited, Ottama, Ontario
[5]Eisinger R, Ruprecht A. (2001), "*Automatic Shape Optimization of Hydro Turbine Components Based on CFD*", Transaction of Emeraldinsight, Vol.6, No.1, pp.101-111
[6]Maryse Francois, Pie Yves Lowys, Gerard Vuillerod (2002), "*Development and Recent Projects for Hooped Pelton Turbine*", Transaction of HYDRO-2002, Turkey, Alstorm
[7]Yodchai Tiaple, Udomkiat Nontakaew (2004), "*The Development of Bulb Turbine for Low Head Storage Using CFD Simulation*", Transaction of ENERGY-BASED.NRTC.GO, publication#1, pp.10-14
[8]B. Zoppe, C. Pellone, T. Maitre, P. Leroy (2006), "*Flow Analysis Inside a Pelton Turbine Bucket*", Transaction of ASME, Vol. 128, pp.500-511
[9]Michael Marek, Thorsten Stoesser, Philip J.W. Roberts, Volker Weitbrecht, Gerhard H. Jirka (2006), "*CFD Modelling of Turbulent Jet Mixing in a Water Storage Tank*", Transaction of UNI-KARLSRUHE, pp.1-10
[10] [16]Zn Zhang , M Casey (2008), "*Experimental Studies of the jet of a Pelton Turbine*", Power and Energy , Mech E Vol. 221 Part A, pp.1181-1189
[11] Bansal R.K. (2005), "*A textbook of Fluid Mechanics and Hydraulic Machines*", Laxmi Publications, New Delhi
[12] S Bharat Krishna and Prof V Ganeshan, "CFD Analysis of Flow through vane swirlers"
[13] Paul Breeze (2005), "*Hydropower: Power Generation Technologies*", pp. 104-121
[14] Peggy Brookshier (2005), "*Hydropower Technology*", U.S. Department of Energy, Idaho, United States
[15] Shamesw I.H. (2002), "*Mechanics of Fluids*", McGraw Hill Publications
[16] Roer E.A. Arndt (2005), "*Hydroelectric Power Stations*", Encyclopaedia of Physical Science and Technology, pp. 489-504.
[17] www.springerlink.com
[18] http://scitation.aip.org
[19] http://www.mathematik.uni-dortmund.de
[20] ANSYS, 2005, CFX-10.0, user manual
[21] User manual from fluent.com